DOI: 10.1002/((please add manuscript number))
Article type: Full Paper

Liquid-Gated Organic Electronic Devices Based on High-Performance Solution-Processed Molecular Semiconductor

*Michele Di Lauro, Marcello Berto, Martina Giordani, Simone Benaglia, Guillaume Schweicher, Dominique Vuillaume, Carlo A. Bortolotti, Yves H. Geerts and Fabio Biscarini**

Dr. Michele Di Lauro, Dr. Marcello Berto, Martina Giordani, Simone Benaglia, Dr. Carlo A. Bortolotti, Prof. Fabio Biscarini.
Dipartimento di Scienze della Vita, Università di Modena e Reggio Emilia, Via Campi 103, 41125 Modena, Italy.
E-mail: fabio.biscarini@unimore.it

Dr. Marcello Berto: Dipartimento di Scienze Biomediche e Chirurgico Specialistiche, Università di Ferrara, Via Fossato di Mortara 17, 44121 Ferrara, Italy.

Martina Giordani: Dipartimento di Scienze Biomediche, Metaboliche e Neuroscienze, Università di Modena e Reggio Emilia, Via Campi 287, 41125 Modena, Italy.

Dr. Guillaume Schweicher, Prof. Yves H. Geerts
Laboratoire de Chimie des Polymères, Faculté des Sciences, Université Libre de Bruxelles (ULB), Boulevard de Triomphe, 1050 Bruxelles, Belgium

Dr. Guillaume Schweicher present address: Optoelectronics Group, Cavendish Laboratory, JJ Thomson Avenue, Cambridge CB3 0HE, United Kingdom

Prof. Dominique Vuillaume
Institute for Electronics Microelectronics and Nanotechnology, CNRS, Université de Lille, Av. Poincaré, F-59652 CEDEX, Villeneuve d'Ascq, France

Keywords: organic transistors; synapstors; organic bioelectronics; PEDOT:PSS; BTBT

Abstract

High mobility organic semiconductors such as [1]Benzothieno[3,2-b]benzothiophene (BTBT) derivatives are potential candidates for ultra-sensitive biosensors. Here 2,7-dioctyl BTBT (C8-BTBT-C8)-based liquid-gated organic electronic devices are demonstrated with two device architectures, viz. Electrolyte-Gated Organic Field-Effect Transistor (EGOFET) and

Synapstor (EGOS), and different electrode materials, viz. gold and and poly-(3,4-ethylenedioxythiophene):poly-styrene sulfonate (PEDOT:PSS). EGOFETs exhibit a mean transconductance of about 45 μS, on a par with literature, and a max value up to 256 μS at the state-of-the-art in aqueous electrolyte ~~as large as 265 μS~~, with a mean product of charge mobility and effective capacitance of about 0.112 $\mu S \cdot V^{-1}$ and 0.044 $\mu S \cdot V^{-1}$ for gold and PEDOT:PSS electrodes, respectively. EGOSs exhibit a dynamic response with 15 ms characteristic timescale with Au electrodes and about twice with PEDOT:PSS electrodes. These results demonstrate a promising route for sensing applications in physiological environment based on fully solution-processed whole-organic electronic devices featuring ultra-high sensitivity and fast response.

1. Introduction

Liquid-gated organic transistors are emerging as ultra-sensitive devices for the detection of bio-markers,[1–3] ions,[4,5] and molecular analytes,[6,7] as well as for the transduction of bioelectrical signals.[8,9] The gate electrode in these devices is immersed in a liquid phase, typically an aqueous electrolytic solution; application of a Gate potential (V_{GS}) results in the build-up of two electrical double layers (at the gate/electrolyte and electrolyte/active material interfaces) which are responsible of charge modulation in the semi-conductive organic layer and of the subsequent change of the source-drain current (I_{DS}). Amongst a variety of architectures used as organic-electronic bio-sensors, the lowest detection levels (i.e. minimum detectable variations in analyte concentration) were obtained with Electrolyte-Gated Organic Field-Effect Transistors (EGOFETs)[1,6,10–12] operated in accumulation mode with pentacene,[1,3,6] α-sexithiophene,[13,14] and poly(3-hexylthiophene-2,5-diyl) (P3HT)[10] channels. Figure 1a shows the schematic layout of EGOFETs. A quantitative estimator of the

sensitivity of a transistor as a sensor is the transconductance g_m defined as the derivative of the transfer characteristics $\partial I_{DS}/\partial V_{GS}$. In the linear regime, the transconductance reads as:

$$g_m = \frac{\partial I_{DS}}{\partial V_{GS}} = \frac{W}{L}\mu C_{eff} V_{DS} \quad (1)$$

In **Equation 1** W and L are channel width and length, C_{eff} is the effective areal capacitance, μ is the charge carrier mobility and V_{DS} is the potential difference between Source and Drain electrodes. Albeit it is not obvious that equation 1, derived for thin film transistors with solid-state dielectrics, can be adopted for EGOFET, this equation hints to the fact that high field-effect mobility is desirable for devising transistors with high sensitivity.

High transconductance in EGOFET-based sensors is ascribed to the intrinsic large capacitive coupling between gate electrode and semiconductor that enables device operations with voltage V_{GS} ranging from a few tens up to a few hundred mV, and yields a large I_{DS} modulation in response to small activity modifications at either the electrolyte/gate or electrolyte/channel interfaces. As suggested by equation 1, transconductance (and hence sensitivity) enhancement can be achieved by maximizing C_{eff} and μ, i.e. by tailoring both the electrolyte composition and the chemical nature and morphology of the semiconductor thin film. The effective capacitance C_{eff}, whose value can be modulated by electrolyte pH and gate voltage,[15] eventually exceeds the one of the electrolyte double layer; however, the apparent charge mobility is observed to generally decrease in liquid-gated architectures (typically in the range 10^{-3}-10^{-4} $cm^2\,V^{-1}\,s^{-1}$)[1,15–17] with respect to solid-state devices with bottom gate.

Within this framework, ~~water-stable~~ high-mobility organic semiconductors operating in aqueous environment would lead to further g_m enhancement and would impact on the performances of electrolyte-gated organic devices also when not operated in EGOFET configuration, as in the case of synapstors.

The organic synapstor (synapse-transistor) is a neuromorphic two-terminal device (two of the transistor terminals are short circuited) that exhibits the electrical signature of a biological synapse.[18,19] In a neural network, synapses modulate signal transmission from a pre-synaptic neuron to a post-synaptic one by delivering neurotransmitters across the synaptic cleft; depending on the spiking frequency at the pre-synaptic neuron, the ionic current at the post-synaptic one can decay (depressing behavior) or rise (facilitating behavior) exponentially. This complex regulation mechanism, termed Short-Term Plasticity (STP), is mimicked by the organic synapstor, which exhibits frequency-dependent modulation of the current evoked by potential pulses at the gate. Frequencies higher or lower than a characteristic frequency υ^{-1} yield depressing or facilitating behavior, respectively. The time scale υ is the result of a network of capacitive and resistive elements that are present in the device. The Electrolyte-Gated Organic Synapstor (EGOS) is the liquid-gated counterpart of Nanoparticle Organic Memory Field-Effect Transistor (NOMFET)[18] and it has recently been demonstrated to operate in contact with a population of neural cells,[20] hinting that hybrid bio-electronic synapses may be possibly useful in prosthetics of damaged neural circuits.[21–23] Also in EGOSs a larger mobility should yield a decrease of the characteristic timescale.

Materials like [1]Benzothieno[3,2-b]benzothiophene (BTBT) derivatives are attractive for high performance organic electronics applications.[24] The material of the present study belongs to 2,7-dialkylated BTBTs whose hole mobility exceeds 10 $cm^2 V^{-1} s^{-1}$ in Organic Thin-Film Transistors (OTFTs)[25–27] and 170 $cm^2 V^{-1}s^{-1}$ as measured with field-induced time-resolved microwave conductivity (FI-TRMC).[28] In addition, they possess other attractive features for interfacing them to living matter: i) ease of synthesis and purification;[29,30] ii) solubility in non-chlorinated organic solvents;[31] iii) ease of processing as thin films;[32–37] iv) low T (≈100°C) post-processing yielding to high molecular order;[38,39] v) limited dynamic

disorder.[40] Further desirable properties for their use in bio-interfacing devices are their ambient stability (a work function of 5.3 eV makes them less prone to oxidative processes),[28] and their transparency in the visible region that allows the exploitation of the spectromicroscopy techniques typically used for the characterization of biological matrices.[41] BTBT OFETs operated in aqueous environment have not been reported to date.

This work demonstrates 2,7-dioctyl BTBT (C8-BTBT-C8) as active material both in EGOFET and in EGOS architecture (**Figure 3**a). The transconductance of the EGOFETs is in the order of tens μS, with a maximum observed value as large as 265 μS, while EGOSs exhibit the fastest time scale (15 ms) observed to date. These figures of merit prompt this BTBT derivative as an attractive material for organic bioelectronics.

Results and discussion

EGOFET and EGOS were fabricated on transparent quartz substrates featuring either metallic (Au) or polymeric electrodes made of poly(3,4-ethylenedioxythiophene): polystyrene sulfonate (PEDOT:PSS). Thin films of C8-BTBT-C8, synthesized according to literature,[29] have been deposited on the test patterns by spin coating and their morphology has been characterized by means of Atomic Force Microscopy (AFM), as shown in Figure 1b and **Figure 2**b. All devices were electrically characterized.

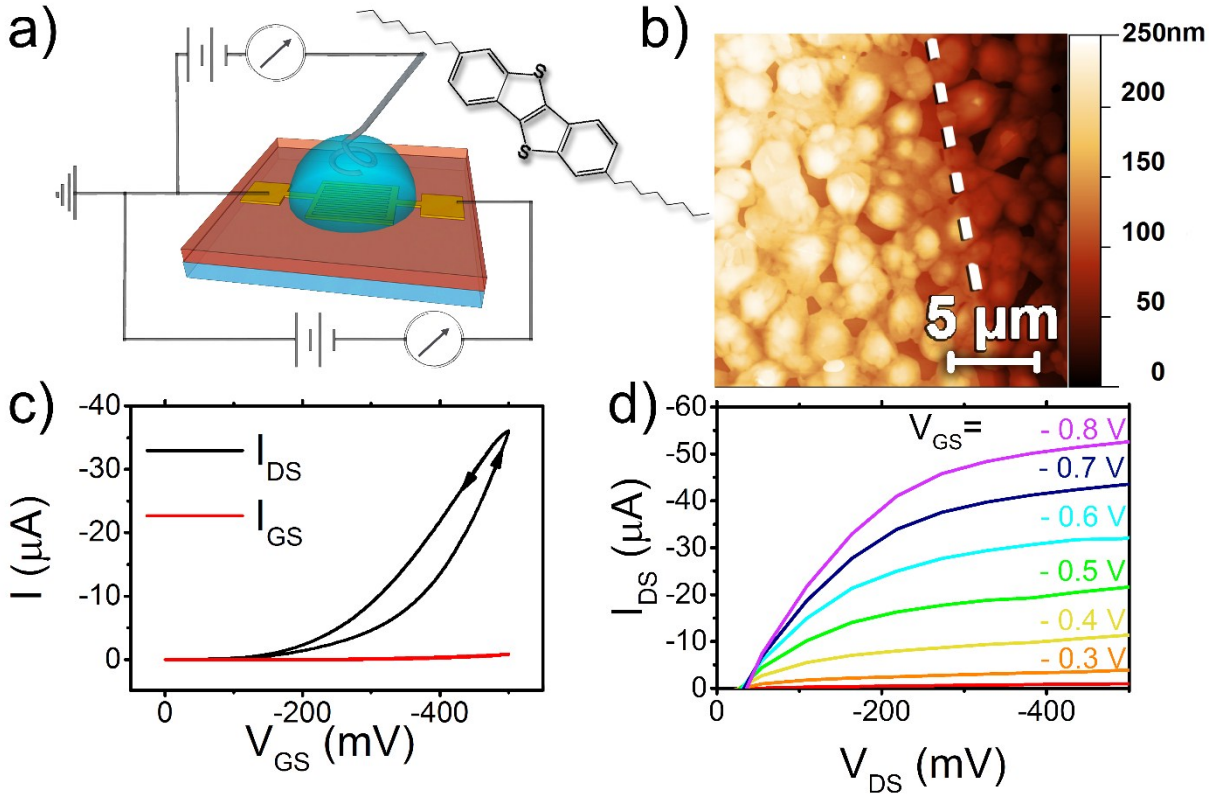

Figure 1. EGOFET featuring gold source and drain: a) schematics of the device depicting electrical connections, gold source and drain, platinum top gate electrode and molecular structure of C8-BTBT-C8; b) 20 µm x 20 µm AFM image of the semiconductor film at the edge (dashed line) between quartz substrate (right) and gold electrode (left); c) transfer characteristic recorded at V_{DS} = -0.2V; d) output characteristics. Transistor parameters averaged over ten devices are V_{th} = -0.356 (± 0.014) V; g_m = 45 (±32) µS and I_{ON}/I_{OFF} = $10^{3.38(\pm 0.06)}$.

Figure 1c and Figure 1d show *I-V* characteristics of EGOFETs featuring Au contacts. The output characteristics in Figure 1d exhibit ohmic response at low voltages and an incomplete plateau at saturation. In these devices, we observed time evolution of the transfer characteristics, with the performances improving upon repeated measurement cycles up to a stability plateau (**Figure S1**, Supporting Information); transistor parameters have been extracted from transfer curves recorded after reaching the stability regime. From the transfer curve in Figure 1c we extracted the best EGOFET parameters obtained in this work V_{th} = -0.360 (± 0.010) V, I_{ON}/I_{OFF} = $10^{3.47(\pm\ 0.04)}$, sub-threshold slope = 79 (± 2) mV dec^{-1} and transconductance g_m = 265 (± 5) µS. These values are comparable to state-of-the-art

parameters of EGOFETs with aqueous electrolyte that are summarized in **Table S1,** Supporting Information.[7,14,17,42–46] It should be noticed that the estimator we choose for comparison is the product of the charge mobility μ by the capacitance C_{eff}, as the device geometry as well as the operation regime may differ. In this respect, our devices with Au electrodes exhibit an average $\mu \cdot C_{eff} = 0.112$ (± 0.080) $\mu S \cdot V^{-1}$, which is in line with most of the experimental values.

The leakage current I_{GS} is more than two orders of magnitude lower than the channel current I_{DS}, and is purely capacitive as solely due to the build-up of the electrical double layer responsible of the gating; no evidence of faradaic reactions was observed in the relevant V_{GS} range. The counterclockwise hysteresis recorded in I_{DS}, and not observed in I_{GS}, points to the asymmetry of the processes of "electrostatic doping and de-doping"[47,48] which should be ascribed to the interaction between the organic semiconductor and the gate-modulated anion distribution and its dynamics. The detailed nature of this modulation is not addressed in our experiment.

PEDOT:PSS test patterns were prototyped from spin cast films subjected to direct laser ablation with a CAD-driven laser scan marker. Figure 2a shows an optical micrograph of the interdigitated PEDOT:PSS source and drain electrodes patterned by laser ablation. Optimization of ablation parameters yields channel lengths as small as 20 µm, resulting in $W/L \approx 1650$. The edge roughness of the electrodes is lower than 1 µm and cannot be resolved within the optical image. The process takes a few minutes and is fully reproducible.

The morphology of the C8-BTBT-C8 film that is spin cast on the PEDOT:PSS test pattern is shown in Figure 2b. The AFM image at the edge between the electrode and the channel resembles that in Figure 1b. The best obtained transfer characteristic for these devices is reported in Figure 2c, yielding V_{th} = -554 (± 2) mV, $I_{ON}/I_{OFF} = 10^{1.68\ (\pm\ 0.03)}$, sub-

threshold slope = 154 (± 1) mV dec^{-1} and transconductance g_m = 24 (± 5) µS. The hysteresis in the source-drain current is much smaller than in the case in Figure 1c. The transistor parameters are perfectly comparable to those extracted from typical devices featuring Au electrodes, as highlighted by the statistical analysis reported in the captions of Figure 1 and Figure 2. From Table S1, our devices with PEDOT:PSS electrodes exhibit an average $\mu \cdot C_{eff}$ = 44 (± 9) nS·V^{-1}, which compares to the average value obtained with Au electrodes.

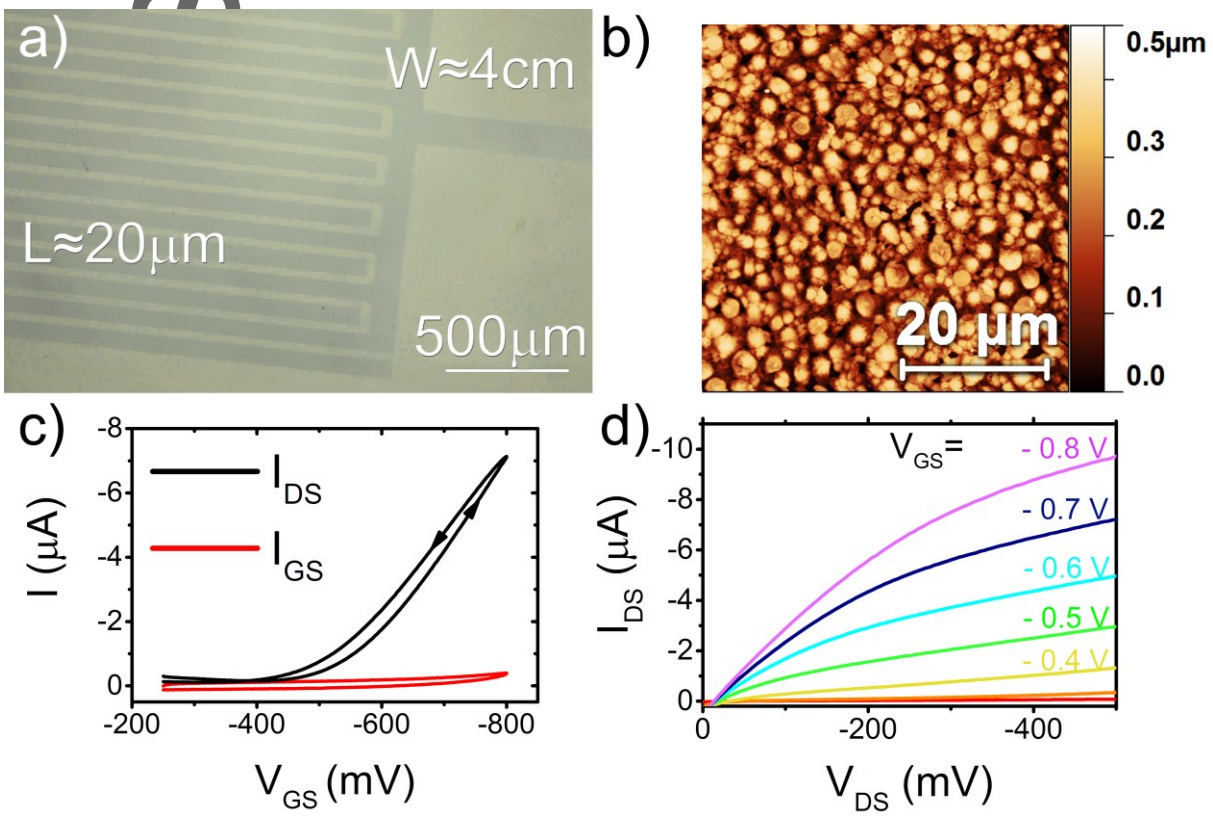

Figure 2. EGOFET featuring PEDOT:PSS source and drain: a) Optical micrograph of interdigitated electrodes on quartz. Final W/L ≈ 1650; b) 50 µm x 50 µm AFM image of the semiconductor film on quartz substrate and PEDOT:PSS; c) transfer characteristic recorded at V_{DS} = -0.3 V; d) output characteristics. Statistical analysis on 5 devices yields: V_{th} = -0.548 (± 0.043) V; g_m = 21.8 (± 4.4) µS and $I_{ON}/I_{OFF} = 10^{3.9(\pm 0.7)}$.

Analysis of the AFM topography yields semiconductor thickness, roughness and morphology scaling parameters of C8-BTBT-C8 films, as described in detail in SI (**Figure S2** and **Table S2**, Supporting Information). We notice that: i) morphology parameters are comparable both on Au and PEDOT:PSS devices; ii) C8-BTBT-C8 topography in the channel does not differ significantly from the one observed on the electrodes (either Au or PEDOT:PSS); iii) larger roughness of PEDOT:PSS electrodes does not result in sizable variations of C8-BTBT-C8 surface area (i.e. only a 3% increase of the surface area moving from Au devices to PEDOT:PSS ones). We do not expect a large influence of the mesoscale surface morphology of C8-BTBT-C8 on resistance and/or capacitance, regardless the different nature of the electrodes. We infer that in our device the EGOFET response is mostly to be ascribed to the C8-BTBT-C8 with minimum influence by the electrodes.

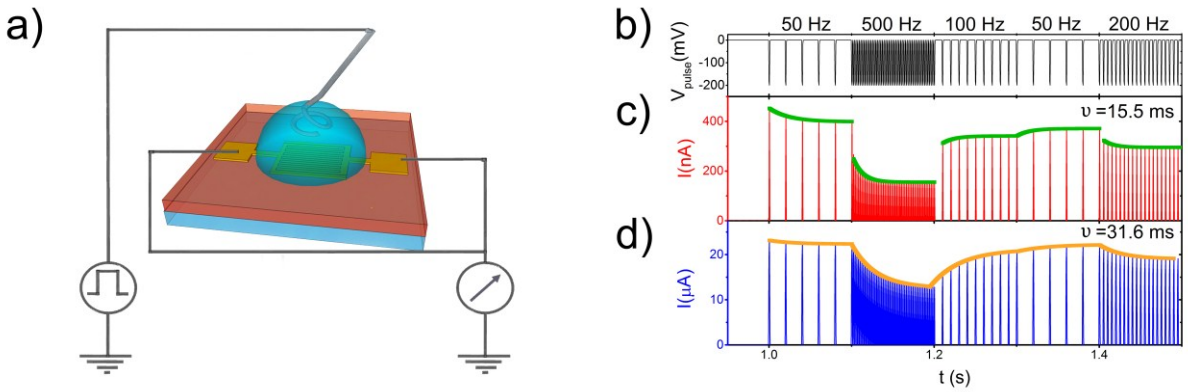

Figure 3. EGOS: a) schematics of the device in which are highlighted electrical connections, gold source and drain electrodes and platinum top gate electrode; b) voltammogram of the input pulse train; STP characterization of the EGOSs with c) Au and d) PEDOT:PSS electrodes. Exponential fits of both the STP responses are shown as green and orange line segments.

EGOS response was also investigated for the two types of electrodes. A schematic representation of EGOS configuration is reported in **Figure 3**a, where source and drain electrodes are both grounded. To investigate STP response the top Pt electrode was pulsed with the sequence of spikes depicted in Figure 3b (50 Hz, 500 Hz, 100 Hz, 50 Hz, 200 Hz;

pulse width = 1 ms, frequency was changed every 100 ms) and the resulting current flowing in the recording electrode was plotted vs time. Current-time, *I-t,* plots are shown in Figure 3c and 3d. Both electrode types yield STP response, although STP in PEDOT:PSS devices exhibits the largest values for absolute current intensity and characteristic time scale, υ: current intensity increases from 452 nA to 23.094 μA and υ from 15.5 ms to 31.6 ms moving from Au to PEDOT:PSS contacts. It is worth noticing that, albeit being about ten times larger than the duration of single action potentials in neurons, the observed timescales are comparable with those of collective physiological events such as brain waves. For instance, the timescale herein reported compares to those typical of β-/γ-waves (20-60 Hz) that are evoked in the brain cortex and are known to be pathognomonic signatures of neuro-degenerative diseases such as Parkinson's disease.[49]

As previously stated, in the relevant voltage range we did not observe the occurrence of faradaic processes, hence the recorded current is the displacement current which is linearly correlated with the effective capacitance of the device.[50] The observed increases of both current intensity and υ (i.e. characteristic time scale of the response of the equivalent circuit of the device) suggest that a higher capacitance is established in the case of PEDOT:PSS electrodes with respect to Au ones. Since the only difference between the two architectures resides in the electrode chemical nature and morphology, while the surface area of C8-BTBT-C8 films does not change significantly, this noticeable change of capacitance hints to the contact interface between the electrodes and the electrolyte, regardless of the presence of the C8-BTBT-C8 film.[15,51] Under this assumption, the marked difference of capacitance can be ascribed to a larger electrolyte-accessible electrodic area in the case of polymeric electrodes, due to hydrophilicity (contact angle $\Theta_{water} \approx 30°$) and porous nature[52,53] in contrast with the rather hydrophobic ($\Theta_{water} \approx 70°$) bulky metallic Au electrodes. Interestingly, as already

observed,[15,51] the organic semiconductor thin film appears perfectly permeable to the solution and especially to ions.

The results of Figure 3 can be rationalized by assuming that the STP response emerges as a consequence of the *RC* equivalent of the device, namely a leaking capacitor resulting from ionic distributions in the electrolyte.[54] This opens unprecedented possibilities for EGOS: by controlling the composition of the electrolyte, the area of the electrodes and the thickness of the semi-conductive film it is possible to finely tune the characteristic time and the magnitude of the STP response. To appreciate the advantage of it, in NOMFET architectures this is done by embedding gold nanoparticles in the semiconductor film, and tuning their size and density.[18] Noticeably, the ms-response timescales that can be achieved for C8-BTBT-C8-based EGOS compares to the timescales reported for optimized NOMFETs in air[19] and outperform the few seconds timescale measured on Au-NP/pentacene EGOS on quartz.[20]

2. Conclusion

This work presented the first liquid-gated organic electronic devices based on BTBT derivatives as active channel material. Both architectures, either with gold or polymeric electrodes, yielded ~~state-of-the-art~~ remarkable transconductance (directly related to sensitivity when the device is operated as sensor) as EGOFET and fast dynamic response (few tens ms scale) as EGOS. The devices response and the ease of the fabrication techniques, with rapid prototyping based on laser patterning of the electrodes, prompt for the development of whole organic and completely solution-processed electronic devices working in accumulation regime in physiological environments. These BTBT-based organic electronic

devices have the potential to impact on ultra-sensitive diagnostics and therapeutic applications.

3. Experimental Section

Gold electrodes: Gold interdigitated electrodes were fabricated on quartz by means of photolithography and lift-off (Fondazione Bruno Kessler FBK, Trento, Italy). They feature channel length L = 15 μm and width W = 30 mm (W/L = 2000).

PEDOT:PSS electrodes: PEDOT:PSS (PH1000, Clevios™) containing 5% DMSO and 0.2% Silquest (3-glycidoxypropyltrimethoxysilane) was deposited onto clean quartz substrates by spin-coating (3 s @ 500 rpm, 30 s @ 2200 rpm) and cured in thermostatic oven for 20 minutes at 120 °C. CAD drawing of source and drain interdigitated electrodes (see **Figure S3**, Supporting Information) was transferred on the resulting film by means of direct laser ablation using a Nd:YAG laser scan marker (λ = 1064 nm), equipped with three inertial micrometrical motors that allow precise (displacement accuracy < 1 μm) control of the sample holder displacement along each of the three axes (ScribaR, Scriba Nanotecnologie Srl, Bologna, Italy).[55]

Semiconductor deposition: Thin films of C8-BTBT-C8 were deposited by spin-coating (30 s @ 3500 rpm; 500 rpm s^{-1}) from a 0.4% w/w solution in chloroform and annealed in a standard thermostat oven at 80°C for 40 minutes.

AFM: Morphological characterization was performed using an NT-MDT SMENA Solver platform (Moscow, Russia); all images were obtained in semi-contact mode and analyzed using Gwyddion 2.43 freeware (http://gwyddion.net/).

Electrical Characterization: Device characterization was performed with an Agilent B2902A. Phosphate buffer saline (PBS) (pH = 7.4; i.e. 40 mM Na_2HPO_4, 10 mM KH_2PO_4) was used as

electrolyte; a Pt wire (ø = 800 μm) immersed in the electrolyte (exposed area = 0.36 cm^2) was used as Gate electrode in EGOFET and as pulsed electrode in EGOS.

Supporting Information
Supporting Information is available from the Wiley Online Library or from the author.

Acknowledgements
We gratefully acknowledge the EU 7th Framework Programme [FP7/2007–2013] under Grant Agreement No. 280772, "Implantable Organic Nanoelectronics (I-ONE-FP7)" project, IT MIUR Bilateral Project IT/SE "Poincaré" (Con il contributo del Ministero dell'Istruzione dell'Università e della Ricerca della Repubblica Italiana), the joint INFM-CNR Project "EOS – organic electronics for innovative measuring instruments" for the support. C.A.B. acknowledges Life Science Department through "FAR2015". G.S. acknowledges postdoctoral fellowship support from the Wiener-Anspach Foundation and The Leverhulme Trust (Early Career Fellowship). This study has been supported by the Belgian National Fund for Scientific Research (FNRS – Project No. 2.4565.11) and by a concerted research action of the French Community of Belgium (ARC Project No. 20061). Y.G. has benefited from a mandate of "Francqui Research Professor (2011–2015)". The help of Mathieu Perrier for the synthesis of C8-BTBT-C8 is greatly acknowledged.

Received: ((will be filled in by the editorial staff))
Revised: ((will be filled in by the editorial staff))
Published online: ((will be filled in by the editorial staff))

References

[1] S. Casalini, A. C. Dumitru, F. Leonardi, C. A. Bortolotti, E. T. Herruzo, A. Campana, R. F. de Oliveira, T. Cramer, R. Garcia, F. Biscarini, *ACS Nano* **2015**, *9*, 5051.

[2] G. Palazzo, D. De Tullio, M. Magliulo, A. Mallardi, F. Intranuovo, M. Y. Mulla, P. Favia, I. Vikholm-Lundin, L. Torsi, *Adv. Mater.* **2015**, *27*, 911.

[3] M. Berto, S. Casalini, M. Di Lauro, S. L. Marasso, M. Cocuzza, D. Perrone, M. Pinti, A. Cossarizza, C. F. Pirri, D. T. Simon, M. Berggren, F. Zerbetto, C. A. Bortolotti, F. Biscarini, *Anal. Chem.* **2016**, *88*, 12330.

[4] M. Sessolo, J. Rivnay, E. Bandiello, G. G. Malliaras, H. J. Bolink, *Adv. Mater.* **2014**, *26*, 4803.

[5] O. Knopfmacher, M. L. Hammock, A. L. Appleton, G. Schwartz, J. Mei, T. Lei, J. Pei, Z. Bao, *Nat. Commun.* **2014**, *5*, 2954.

[6] S. Casalini, F. Leonardi, T. Cramer, F. Biscarini, *Org. Electron. physics, Mater. Appl.* **2013**, *14*, 156.

[7] M. Y. Mulla, E. Tuccori, M. Magliulo, G. Lattanzi, G. Palazzo, K. Persaud, L. Torsi, *Nat. Commun.* **2015**, *6*, 6010.

[8] T. Cramer, a. Campana, F. Leonardi, S. Casalini, a. Kyndiah, M. Murgia, F. Biscarini, *J. Mater. Chem. B* **2013**, *1*, 3728.

[9] X. Strakosas, M. Bongo, R. M. Owens, *J. Appl. Polym. Sci.* **2015**, *132*, 1.

[10] M. Magliulo, A. Mallardi, R. Gristina, F. Ridi, L. Sabbatini, N. Cioffi, G. Palazzo, L. Torsi, *Anal. Chem.* **2013**, *85*, 3849.

[11] M. L. Hammock, O. Knopfmacher, B. D. Naab, J. B.-H. Tok, Z. Bao, *ACS Nano* **2013**, *7*, 3970.

[12] L. Kergoat, B. Piro, M. Berggren, M.-C. Pham, A. Yassar, G. Horowitz, *Org. Electron.* **2012**, *13*, 1.

[13] F. Buth, D. Kumar, M. Stutzmann, J. A. Garrido, *Appl. Phys. Lett.* **2011**, *98*, DOI 10.1063/1.3581882.

[14] F. Buth, A. Donner, M. Sachsenhauser, M. Stutzmann, J. A. Garrido, *Adv. Mater.* **2012**, *24*, 4511.

[15] M. Di Lauro, S. Casalini, M. Berto, A. Campana, T. Cramer, M. Murgia, M. Geoghegan, C. A. Bortolotti, F. Biscarini, *ACS Appl. Mater. Interfaces* **2016**, *8*, 31783.

[16] M. Magliulo, A. Mallardi, M. Y. Mulla, S. Cotrone, B. R. Pistillo, P. Favia, I. Vikholm-Lundin, G. Palazzo, L. Torsi, *Adv. Mater.* **2013**, *25*, 2090.

[17] H. Toss, C. Suspène, B. Piro, A. Yassar, X. Crispin, L. Kergoat, M.-C. Pham, M.

Berggren, *Org. Electron.* **2014**, *15*, 2420.

[18] F. Alibart, S. Pleutin, D. Guérin, C. Novembre, S. Lenfant, K. Lmimouni, C. Gamrat, D. Vuillaume, *Adv. Funct. Mater.* **2010**, *20*, 330.

[19] S. Desbief, A. Kyndiah, D. Guérin, D. Gentili, M. Murgia, S. Lenfant, F. Alibart, T. Cramer, F. Biscarini, D. Vuillaume, *Org. Electron.* **2015**, *21*, 47.

[20] S. Desbief, M. di Lauro, S. Casalini, D. Guerin, S. Tortorella, M. Barbalinardo, A. Kyndiah, M. Murgia, T. Cramer, F. Biscarini, D. Vuillaume, *Org. Electron.* **2016**, *38*, 21.

[21] S. Saïghi, C. G. Mayr, T. Serrano-Gotarredona, H. Schmidt, G. Lecerf, J. Tomas, J. Grollier, S. Boyn, A. F. Vincent, D. Querlioz, S. La Barbera, F. Alibart, D. Vuillaume, O. Bichler, C. Gamrat, B. Linares-Barranco, *Front. Neurosci.* **2015**, *9*, 1.

[22] P. Gkoupidenis, N. Schaefer, X. Strakosas, J. A. Fairfield, G. G. Malliaras, *Appl. Phys. Lett.* **2015**, *107*, 6.

[23] T. Tuma, A. Pantazi, M. Le Gallo, A. Sebastian, E. Eleftheriou, *Nat. Nanotechnol.* **2016**, *11*, 693.

[24] K. Takimiya, I. Osaka, T. Mori, M. Nakano, *Acc. Chem. Res.* **2014**, *47*, 1493.

[25] G. Schweicher, Y. Olivier, V. Lemaur, Y. H. Geerts, *Isr. J. Chem.* **2014**, *54*, 595.

[26] G. Schweicher, V. Lemaur, C. Niebel, C. Ruzié, Y. Diao, O. Goto, W. Lee, Y. Kim, J. Arlin, J. Karpinska, A. R. Kennedy, S. R. Parkin, Y. Olivier, S. C. B. Mannsfeld, J. Cornil, Y. H. Geerts, Z. Bao, **2015**, 1.

[27] R. Janneck, F. Vercesi, P. Heremans, J. Genoe, C. Rolin, *Adv. Mater.* **2016**, 1.

[28] Y. Tsutsui, G. Schweicher, B. Chattopadhyay, T. Sakurai, J.-B. Arlin, C. Ruzié, A. Aliev, A. Ciesielski, S. Colella, A. R. Kennedy, V. Lemaur, Y. Olivier, R. Hadji, L. Sanguinet, F. Castet, S. Osella, D. Dudenko, D. Beljonne, J. Cornil, P. Samorì, S. Seki,

Y. H. Geerts, *Adv. Mater.* **2016**, 7106.

[29] H. Ebata, T. Izawa, E. Miyazaki, K. Takimiya, M. Ikeda, H. Kuwabara, T. Yui, *J. Am. Chem. Soc.* **2007**, *129*, 15732.

[30] C. Ruzié, J. Karpinska, A. R. Kennedy, Y. H. Geerts, *J. Org. Chem.* **2013**, *78*, 7741.

[31] C. Liu, Y. Li, Y. Xu, T. Minari, S. Li, K. Takimiya, K. Tsukagoshi, *Org. Electron. physics, Mater. Appl.* **2012**, *13*, 2975.

[32] T. Uemura, Y. Hirose, M. Uno, K. Takimiya, J. Takeya, *Appl. Phys. Express* **2009**, *2*, 2.

[33] H. Minemawari, T. Yamada, H. Matsui, J. Tsutsumi, S. Haas, R. Chiba, R. Kumai, T. Hasegawa, *Nature* **2011**, *475*, 364.

[34] M. Treier, J.-B. Arlin, C. Ruzié, Y. H. Geerts, V. Lemaur, J. Cornil, P. Samorì, *J. Mater. Chem.* **2012**, *22*, 9509.

[35] M. Dohr, O. Werzer, Q. Shen, I. Salzmann, C. Teichert, C. Ruzié, G. Schweicher, Y. H. Geerts, M. Sferrazza, R. Resel, *Chemphyschem* **2013**, *14*, 2554.

[36] G. Gbabode, M. Dohr, C. Niebel, J. Y. Balandier, C. Ruzié, P. Négrier, D. Mondieig, Y. H. Geerts, R. Resel, M. Sferrazza, *ACS Appl. Mater. Interfaces* **2014**, *6*, 13413.

[37] D. He, Y. Zhang, Q. Wu, R. Xu, H. Nan, J. Liu, J. Yao, Z. Wang, S. Yuan, Y. Li, Y. Shi, J. Wang, Z. Ni, L. He, F. Miao, F. Song, H. Xu, K. Watanabe, T. Taniguchi, J.-B. Xu, X. Wang, *Nat. Commun.* **2014**, *5*, 5162.

[38] H. Iino, J. Hanna, *Adv. Mater.* **2011**, *23*, 1748.

[39] H. Iino, T. Usui, J.-I. Hanna, *Nat. Commun.* **2015**, *6*, 6828.

[40] S. Illig, A. S. Eggeman, A. Troisi, L. Jiang, C. Warwick, M. Nikolka, G. Schweicher, S. G. Yeates, Y. Henri Geerts, J. E. Anthony, H. Sirringhaus, *Nat. Commun.* **2016**, *7*, 10736.

[41] M. El Gemayel, K. Börjesson, M. Herder, D. T. Duong, J. a Hutchison, C. Ruzié, G. Schweicher, A. Salleo, Y. Geerts, S. Hecht, E. Orgiu, P. Samorì, *Nat. Commun.* **2015**, *6*, 6330.

[42] Q. Zhang, F. Leonardi, S. Casalini, I. Temiño, M. Mas-Torrent, *Sci. Rep.* **2016**, *6*, 39623.

[43] F. Leonardi, S. Casalini, Q. Zhang, S. Galindo, D. Guti??rrez, M. Mas-Torrent, *Adv. Mater.* **2016**, 10311.

[44] R. Porrazzo, S. Bellani, A. Luzio, E. Lanzarini, M. Caironi, M. R. Antognazza, *Org. Electron. physics, Mater. Appl.* **2014**, *15*, 2126.

[45] D. Wang, V. Noël, B. Piro, *Electronics* **2016**, *5*, 9.

[46] C. Suspène, B. Piro, S. Reisberg, M.-C. Pham, H. Toss, M. Berggren, A. Yassar, G. Horowitz, *J. Mater. Chem. B* **2013**, *1*, 2090.

[47] M. Egginger, S. Bauer, R. Schwödiauer, H. Neugebauer, N. S. Sariciftci, *Monatshefte für Chemie - Chem. Mon.* **2009**, *140*, 735.

[48] P. D'Angelo, P. Stoliar, T. Cramer, A. Cassinese, F. Zerbetto, F. Biscarini, *Appl. Phys. A Mater. Sci. Process.* **2009**, *95*, 55.

[49] F. Lopes da Silva, *Electroencephalogr. Clin. Neurophysiol.* **1991**, *79*, 81.

[50] L. Bard, A.; Faulkner, *Electrochemical Methods: Fundamentals and Applications*, **2001**.

[51] N. Lago, A. Cester, N. Wrachien, M. Natali, S. D. Quiroga, S. Bonetti, M. Barbato, A. Rizzo, E. Benvenuti, V. Benfenati, M. Muccini, S. Toffanin, G. Meneghesso, *Org. Electron.* **2016**, *35*, 176.

[52] J. Newman, W. Tiedemann, *AIChE J.* **1975**, *21*, 25.

[53] A. Elschner, S. Kirchmeyer, W. Lovenich, U. Merker, K. Reuter, *PEDOT: Principles*

and Applications of an Intrinsically Conductive Polymer, CRC Press, **2010**.

[54] J. N. Israelachvili, *Intermolecular and Surface Forces: Revised Third Edition*, **2011**.

[55] M. Giordani, M. Di Lauro, M. Berto, C. A. Bortolotti, D. Vuillaume, H. L. Gomes, M. Zoli, F. Biscarini, in *Proc. SPIE* (Eds.: I. Kymissis, R. Shinar, L. Torsi), **2016**, p. 99440P.

The first demonstration of benzothieno-benzothiophene (BTBT) derivatives in liquid-gated organic electronic devices is presented. Two architectures exploiting both organic and metallic electrodes are validated. Electrolyte-Gated Organic Field-Effect Transistors (EGOFETs) based on thin films of a solution processed dialkylated BTBT show state-of-the-art electrical performances and fast dynamic response when measured as Electrolyte-Gated Organic Synapstors (EGOSs).

Keywords organic transistors, synapstors, organic bioelectronics, PEDOT:PSS, BTBT

Authors Michele Di Lauro, Marcello Berto, Martina Giordani, Simone Benaglia, Guillaume Schweicher, Dominique Vuillaume, Carlo A. Bortolotti, Yves H. Geerts and Fabio Biscarini*

Title: Liquid-Gated Organic Electronic Devices Based on High-Performance Solution-Processed Molecular Semiconductor